ORIGINAL PAPER

A. Chopelas · G. Serghiou

Spectroscopic evidence for pressure-induced phase transitions in diopside

Abstract Raman spectra of diopside were collected from atmospheric pressure to 71 GPa. The pressure dependences of 22 modes were determined. Changes occurred in the spectra at three different pressures. First, at approximately 10 GPa, the two Raman modes at 356 and 875 cm^{-1} disappeared, while the mode at 324 cm^{-1} split into two modes, diverging at this pressure with significantly different pressure shifts; second, at approximately 15 GPa, a small (1 to 2 cm^{-1}) drop in several of the frequencies was observed accompanied by changes in the pressure dependency of some of the modes; and third, above 55 GPa, the modes characteristic of chains of tetrahedrally coordinated silicon disappeared, while those for octahedrally coordinated silicon appeared. The first change at 10 GPa appears to be a $C2/c$ to $C2/c$ transition involving a change in the Ca coordination. The third change above 55 GPa appears to be a change in the silicon coordination. At 15 GPa, it is suggested that a change in compressional mechanism takes place.

Keywords Diopside · Clinopyroxene · Raman spectroscopy · High pressure

Introduction

Diopside, CaMgSi$_2$O$_6$, one of the major components in the upper mantle, progressively transforms to a garnet phase over a pressure range at temperatures found in the transition zone in the mantle. Compared to forsterite, Mg$_2$SiO$_4$, far fewer thermal and elastic properties have been measured for diopside and most of these

under-ambient or near-ambient conditions. Modeling the chemical and thermal properties of the mantle with these data requires extrapolation to mantle conditions. In general, this yields satisfactory results. However, if there are changes in phase or compressional mechanism, the extrapolation may be invalid. In this paper, we demonstrate that diopside undergoes three such changes, two at relatively modest pressures and one at very high pressures (above its stability field) at room temperature. Similar behavior has been found in a number of other minerals, so the study of the changes in diopside will help us understand how to better extrapolate physical properties to mantle conditions. In a subsequent paper, the spectroscopic data taken here will be used as a basis for making estimates of the heat capacity, entropy, and thermal expansivity at high pressures and temperatures using a quasiharmonic model and statistical methods. The effects of the changes versus pressure discussed here on extrapolation will also be shown.

Experimental details

Raman spectra of diopside from DeKalb, NY, (Levein et al. 1979) were measured at ambient and high pressures and 22 °C. For the high-pressure measurements, approximately 40-μm chips of diopside, μm-sized ruby chips, and either a 4:1 methanol:ethanol mixture or argon as a pressure medium were confined by a stainless steel gasket with a 120-μm diameter hole. (Note: alcohol was used until the gas loader was constructed. No differences in spectral results were noted in the pressure region where both media were used, see below.) The 250-μm culet diamonds were mounted in a diamond cell of our own design on tungsten carbide seats with a large aperture (≈f/2), which allows for collection of a significant cross-section of the weak Raman signal. Results from using both methanol:ethanol mixtures and argon as pressure media concurred with one another. In studies of other minerals, such as enstatite or forsterite, changes such as those described in this article occurred at entirely different pressures. Furthermore, argon, ethanol–methanol mixtures, ethanol–methanol–water mixtures, and KBr as pressure media all yielded the same results to 20 GPa, the limit of some of the tests. Thus, these changes are inherent in the sample and are medium-independent.

Pressures were measured before and after recording the sample spectra; maximum differences observed did not exceed 1% of the

A. Chopelas (✉)
Department of Physics,
University of Washington,
PO Box 351560 Seattle,
Washington 98195-1560, USA
E-mail: chopelas@phys.washington.edu

G. Serghiou
Max Planck Institut für Chemie,
Mainz, 55020 Germany

confining pressure. The Raman spectra of diopside were excited with typically less than 25 mW of the 457.9-nm line of an argon laser, which was kept to the minimum power needed in order to avoid heating the sample due to light absorption. No peak broadening or shifting due to heating was observed. The laser light entered the diamond cell at an incident angle of approximately 25° and was focused to approximately 10-μm diameter in the sample. The signal was collected in a backscattering geometry with an f/2 lens and focused into an ISA U1000 double monochromator, which was equipped with a photon-counting detection system. Typical spectral resolution was 1 cm⁻¹. All spectra were recorded in a climate-controlled environment, with temperatures typically 293 ± 1 K, in order to prevent drift in monochromator calibration. Raman spectra were taken on both increasing and decreasing pressure. The uncertainties in the frequencies at ambient conditions are ±0.5 cm⁻¹ and at high pressure ±1 cm⁻¹ due to the decrease in signal-to-noise ratio. Spectra were collected with a range of frequencies from 40 to 1200 cm⁻¹.

Results

Diopside is a chain silicate that crystallizes in the $C2/c$ space group with two formula units ($CaMgSi_2O_6$) per unit cell. There are 60 normal modes of vibration at any one point in the Brillouin zone, 30 of which are Raman-active, 14 Ag and 16 Bg. Applying factor group analysis to these modes, we obtain 20 modes that are primarily internal motions of the Si–O chain, while 4 are external chain motions and 6 are cation translations. There are two distinct cation sites, the smaller, M1, site here containing Mg and the larger, M2, site containing Ca. There is only one crystallographically distinct silicate chain in diopside with a repeat unit of two and is nearly fully extended with an O(3)–O(3)–O(3) bond angle of 165° (e.g., Levein and Prewitt 1981). The tetrahedrally coordinated corner-shared silicate chains are parallel to the c axis. Chains of edge-shared MgO_6 octahedra and CaO_8 dodecahedra run parallel to the silicate chains. The calcium site is quite distorted with four long and four short bonds, with the average bond length of the two differing by 12%. It was observed at low pressures that the Ca dodecahedron became more regular upon compression (Levein and Prewitt 1981), but the highest pressure of this study was only 5.3 GPa.

Our 1-atm diopside spectra agree very closely with previous results (Etchepare 1970) with only a 1 to 2 cm⁻¹ difference in peak frequencies between that study and this one. Not all the peaks expected by symmetry considerations were found previously, despite the high quality of the spectra (Table 1). A very weak peak at 960 cm⁻¹, probably of Bg symmetry, may be the one missing peak. Prominent peaks of unknown symmetry were found at 886 and 1033 cm⁻¹ in the high-pressure experiments. The 886 cm⁻¹ mode disappeared at higher pressures while the 1033 cm⁻¹ mode did not. The 886 cm⁻¹ mode reappeared at low pressures. It is not clear what the origin of these two modes is, but the 1033 cm⁻¹ mode due to its broadness could well be a combination mode, while the 886 cm⁻¹ mode appears to be a fundamental.

The vibrational modes of diopside in relationship to its structure and bonding characteristics are generally

Table 1 Summary of 1-atm Raman frequencies of diopside

Ag modes (cm⁻¹)		Bg modes (cm⁻¹)	
This work	(Etchepare 1970)	This work	(Etchepare 1970)
140	140	115	118
183	182	166	169
234	235	196	198
257	256	231	232
325	326	303	305
362	360?	–	328
391	390	357	358
509	508?	393	395
531	530	466	468
668	668	517	517
857	858	561	560
1015	1016	708	710
1033?		917	920
1050	1050	960	
		–	1015?
		–	1048?

classified into three regimes. The regime below 500 cm⁻¹ consists of modes associated with cation translations as well as longer-wavelength lattice modes. The peaks in the midfrequency region between 500 and 800 cm⁻¹ are associated with Si–O–Si intertetrahedral stretching and bending modes. The bands at higher wavenumbers are associated with Si–O stretching modes of the nonbridging oxygens in the silicon tetrahedra. This scheme is useful when there are significant differences in the bond strengths in two different parts of the structure, as is the case in diopside. The internal modes can be easily assigned since they are separated from the lattice modes and they provide structural information directly. For example, in pyroxenes and other structures with Si–O–Si bridges, intense modes are found at about 700 cm⁻¹, unlike in spectra of other silicates such as olivines and garnets. The 700-cm⁻¹ mode is associated with symmetric stretching of the silicon–oxygen bridge. However, specific assignments are difficult for modes below 500 cm⁻¹ since all vibrational modes are really whole-lattice modes and in this region, extensive mixing of motions occurs since the frequencies of the different motions are similar in this area. Thus, although by symmetry considerations there are three modes due to the cation translations, they cannot be distinguished by their high-pressure behavior. It would be expected that they have the highest pressure dependence, since a cation translation occurs in the portion of the structure that compresses the most. As will be shown, there are several modes with a large pressure shift and an unambiguous assignment of modes to atomic motions cannot be made.

High-pressure behavior

Raman spectra of $CaMgSi_2O_6$ upon compression (Fig. 1a) reveal the following distinct changes: By 4.2 GPa, the intensities of the dominant modes at 390 and 875 cm⁻¹ begin decreasing. By 10.4 GPa, these
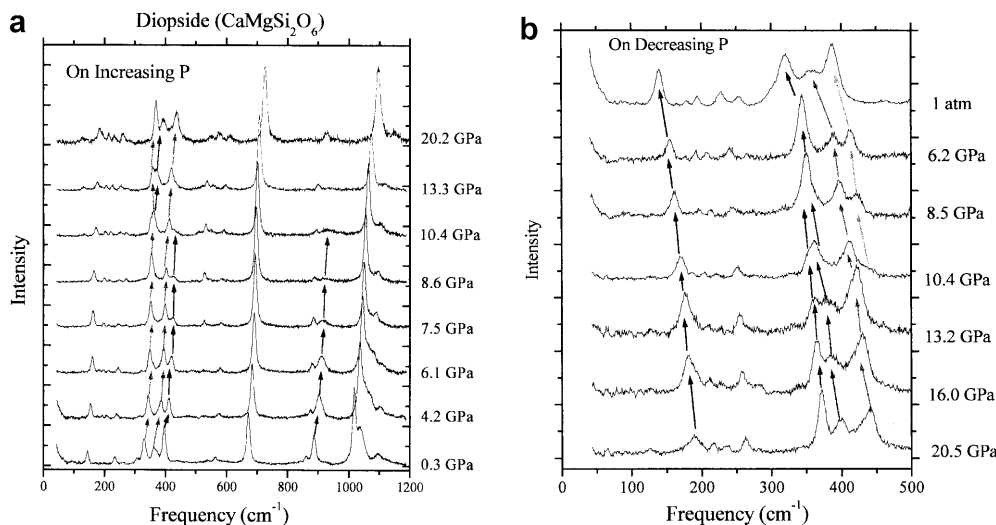
Fig. 1 **a** Raman spectrum of diopside from 0.3 to 20.2 GPa. The *arrows* follow the peaks that change from 6.1 to 10.4 GPa. At 10.4 GPa, the peak at 390 cm^{-1} disappears and that at 325 cm^{-1} splits, so the final spectrum strongly resembles the initial spectrum, suggesting that both are the same symmetry. **b** Raman spectrum of modes below 500 cm^{-1} in diopside on decreasing pressure from 20.5 GPa to ambient pressure. The mode at 325 cm^{-1} reemerges and the mode at 390 cm^{-1} reappears at the same pressures as on compression (10.4 GPa). The *arrows* are guides for the eye. There is little obvious hysteresis

modes have disappeared while another intense mode appears near the 325 cm^{-1} mode, making it appear as if the modes are splitting. The resulting Raman spectrum at 20.2 GPa is nearly identical to the original spectrum at 1 atm, suggesting that the symmetry has not changed and no significant bond breakage and/or new bonds formed. These effects are completely reversible without hysteresis (Fig. 1b) as seen in the decompression cycle. It is unlikely that the mode emerging from under the 325 cm^{-1} mode above 10 GPa was present in the 1-atm spectrum because the intensity and pressure dependence would place it at about 315 cm^{-1} at 1 atm, far enough away from any of the other modes to be easily resolved.

A plot of mode positions versus pressure (Fig. 2a–d; Table 1) does not reveal any unusual behavior or abrupt changes in slope until about 15 GPa, with the exception of the splitting of the 325 cm^{-1} mode. An expansion of the scale around this pressure for the mode at 365 cm^{-1} reveals that the frequency has dropped slightly before continuing on to higher frequencies at a slightly different pressure dependency as pressure was increased (Fig. 3). This effect was seen clearly in both methanol–ethanol and argon pressure media and was fully reproducible on pressure cycling. This small change exhibits hysteresis: the frequencies are somewhat lower on decompression below 15 GPa than they were on compression (Fig. 4).

The pressure dependencies (Table 2) show a clear division in frequency. Above 500 cm^{-1}, the mode Grüneisen parameters $[\gamma_i = (\partial \ln v/\partial \ln V)_T]$ are significantly lower than below. Above 500 cm^{-1}, they average about 0.65, whereas below they average 1.4.

Since the compression of diopside is mostly taken up by the shortening of the cation oxygen bonds and collapsing the voids, accompanied by a decrease in the O3–O3–O3 bond angle in the silicate chain (Levein and Prewitt 1981), the lattice modes below 500 cm^{-1} should show the largest pressure shift. This has also been observed for a number of minerals, including orthoenstatite, forsterite, and garnets (e.g., Chopelas 1990; Chopelas 1999), the major constituents of the upper mantle.

As mentioned previously, the symmetry analysis of diopside yields three modes that should be associated with cation translations. By examination of the mode γ's, it is clear that there are not just three modes with high values but six to seven in the range one would expect for cation translation (typically 1.1 and higher) and the pressure dependence of only 18 of the 30 Raman-active modes was measured. Thus, there is a great deal of mode mixing, as has been observed for other minerals (e.g., Chopelas 1991; Hofmeister and Chopelas 1991), making it impossible to make discrete mode assignments, as mentioned previously. The pressure dependencies in Table 2 form the basis for changing the density of states model for the calculation of thermodynamic properties of diopside at elevated pressure, which is presented in a subsequent paper.

Discussion

In looking for a likely cause for the 10.4-GPa change observed in the diopside spectra, it is noted that the highest pressure spectra (Fig. 1a) seem nearly the same as the ambient pressure spectra, making it appear that the symmetry has not changed during this "transition". Such a phase transition is possible, since pyroxene crystallizes into three $C2/c$ structures (Hugh-Jones et al. 1994). These are (1) a high-temperature form in which the silicate chain is nearly fully extended with an O3–O3–O3 bond angle of above 170° and the M2 (larger cation site) is dodecahedrally coordinated with nearly all the same bond lengths, (2) a high-pressure form in which
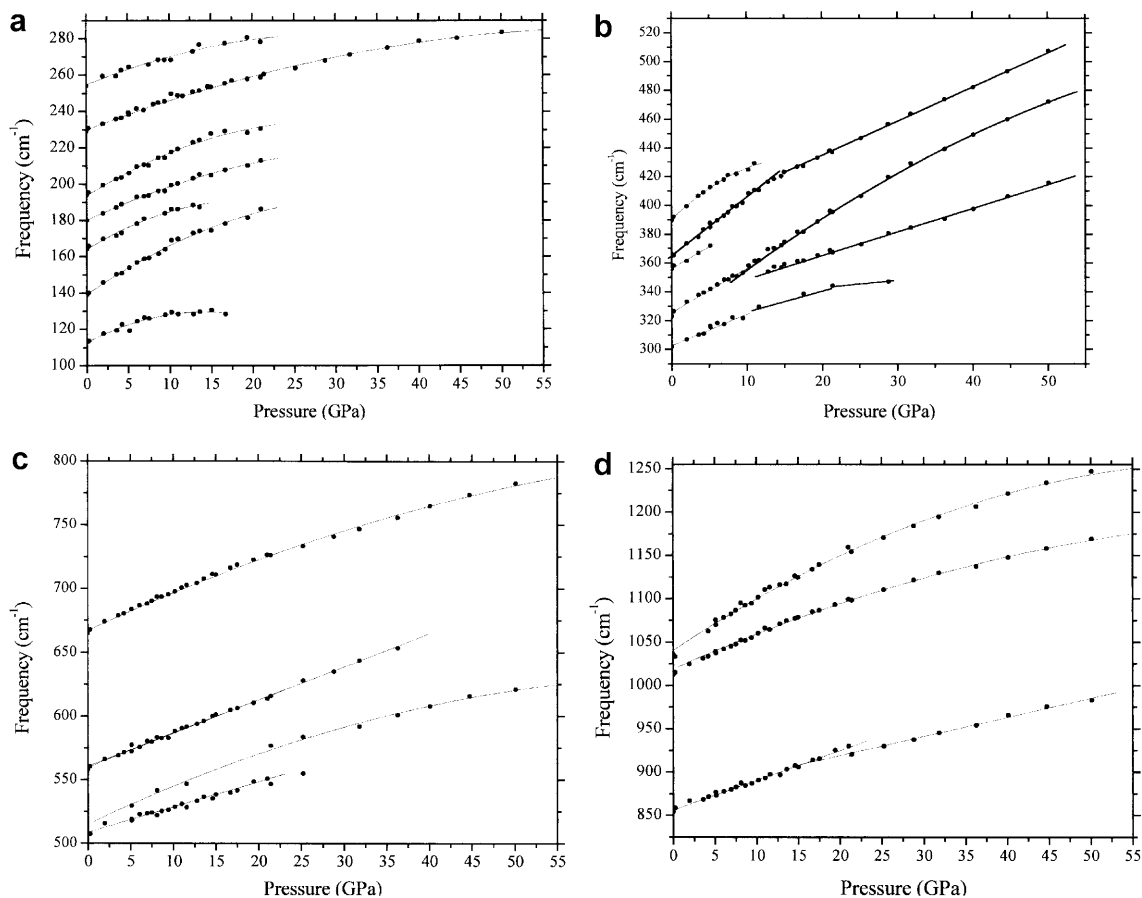
Fig. 2a–d Plot of the Raman mode frequencies versus pressure on increasing pressure. **a** Plot of the frequencies between 100 and 300 cm^{-1}. Missing data above 20 GPa for these modes are due to change in spectrometer and detector system. **b** Plot of the frequencies between 300 and 500 cm^{-1}. In this plot it is evident that the mode at 325 cm^{-1} splits above 10 GPa and the mode at 390 cm^{-1} disappears. **c** Plot of the frequencies between 500 and 800 cm^{-1}. **d** Plot of the frequencies above 800 cm^{-1}. The data taken on decreasing pressure were omitted for clarity but follow exactly the same trends except around 16 GPa (Fig. 3)

the silicate chain is substantially kinked with an O3–O3–O3 angle of under 135° and an octahedrally coordinated M2 site as found in the high-pressure MgSiO$_3$ form of clinoenstatite, and (3) the room-temperature diopside structure in which the silicate chain is only mildly kinked with an O3–O3–O3 bond angle of 166° and a dodecahedrally coordinated M2 site with four short and four long M2–O bonds. Here, it would be possible for diopside to change from structure (3) above to structure (2), even though the low-pressure single-crystal data suggest that the calcium dodecahedron becomes more regular and less distorted at low pressures (Levein and Prewitt 1981). The highest pressure of that study was the lowest pressure in which the Raman spectra started to change.

Evidence for a possible structural change in pyroxenes that fit this criterion is found in recent single-crystal high-pressure X-ray studies of other pyroxenes (Downs et al. 1999). Here, intensity data were collected to obtain atom locations, from which electron density or bonding is deduced. Changes in the data occurring when this pyroxene was compressed show subtle changes in the bonding in the octahedrally coordinated cations. As pressure was increased, the cation bonds shifted from one oxygen along the silicate chain to another, causing subtle changes in structure. Such changes would hardly affect the Raman spectrum but could cause changes such as those seen here. In diopside, it is likely that this shift may be one in which the calcium coordination is reduced to six, making it more similar in structure to high-pressure clinoenstatite. There are some lines of evidence that suggest that the calcium does indeed change bonding. First, the spectrum at about 16 GPa strongly resembles that of MgSiO$_3$ high clinopyroxene, another $C2/c$ pyroxene where both M1 and M2 cations are octahedrally coordinated and the O3–O3–O3 bonding angle is about 133°. Second, in Cr^{3+}-doped diopside, a sharp-lined fluorescence at about 685 nm similar to that found in ruby appears at about 3 GPa upon compression. This type of fluorescence requires an octahedrally coordinated d^3 cation. Since it is likely that trivalent chromium substitutes at the smaller M1 (Mg) site (R.T. Downs, personal communication, 2001), it appears that this site goes from a low-spin to a high-spin state. At 7.5 GPa, a second sharp line fluorescence peak appears at about 688 nm and grows in intensity upon increasing pressure. At 10.5 GPa, the second higher-energy peak
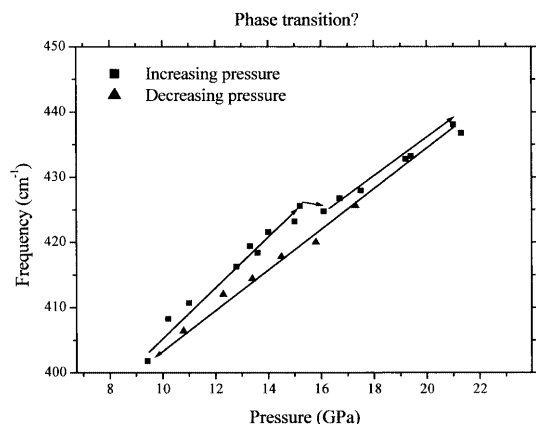
Fig. 3 Enlargement of the 365-cm^{-1} mode versus pressure around 16 GPa, showing a small but resolvable (and reproducible) dip in frequency. On reducing the pressure, the frequency was lower but then returned to the same trend established upon compression. Most, but not all, of the modes displayed this behavior. This was observed in both pressure media, the methanol–ethanol mixture and argon
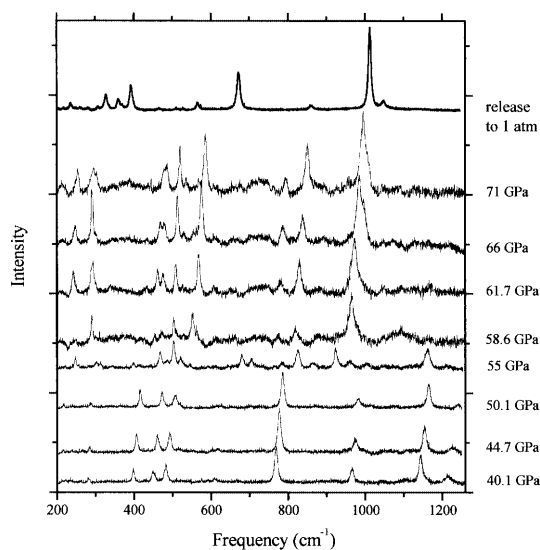

Fig. 4 Raman spectrum of diopside to 71 GPa. Above 50 GPa, the diopside spectrum changes dramatically where the intense modes characteristic of diopside disappear and several new modes appear. The most intense of these modes at around 900 cm^{-1} is at nearly the same frequency as the most intense mode found in magnesium silicate ilmenite (Fig. 5), suggesting that silicon has changed from four-fold to six-fold coordination

Table 2 Pressure dependence of the Raman modes of diopside. The frequencies listed under ν_0 are those returned by the least squares regression to a line or second-order polynomial of the data shown in Fig. 3a-d. The data above 16 GPa were not used in the fits

Frequency (cm^{-1})	ν_0 (cm^{-1})	$d\nu/dP$ (cm^{-1}/GPa)	$d^2\nu/dP^2$ (cm^{-1}/GPa^{-2})
113	112.8	2.36	−0.083
139	139.2	3.17	−0.047
164	164.1	2.80	−0.073
180	180	2.16	−0.029
194	193.6	2.88	−0.051
229	229.1	2.11	−0.033
254.5	254.5	1.87	−0.031
303	302.7	2.17	
—	315.0	4.25	−0.022
325	324.6	3.356	
332	332.4	1.643	
356	356.4	2.98	
365	365.2	4.01	
390	390.2	5.01	−0.154
509	508.8	1.98	
515	515.1	3.19	−0.022
560	559.8	2.65	
667	666.7	3.30	−0.022
856	856.3	3.43	
875	875.2	2.20	
1016	1015.9	4.14	
1033	1033.3	7.45	−0.077

compared to those below this pressure. It is not clear exactly what this phenomenon could be, but it may be related to either (1) the suggested change in bonding at the calcium site or (2) the disproportionation observed in diopside at about this pressure and higher temperatures. In either case, further investigation is required to explain the nature of the observations in the Raman spectrum.

Upon further compression of diopside, the spectrum does not change except to shift frequencies to higher values until over 50 GPa. Here, the modes characteristic of diopside disappear entirely and a spectrum whose most dominant peak is about 950 cm^{-1} appears. Such a spectrum strongly suggests a change in bonding from tetrahedrally to octahedrally coordinated silicon. A comparison of the spectrum of diopside with that of magnesium silicate ilmenite (Fig. 5) shows that the ilmenite spectrum resembles that of diopside compressed to the highest pressures in this study (71 GPa). A comparison of the position and pressure shifts of the most dominant peak in ilmenite to that in the high-pressure phase of diopside shows that they are very similar (Serghiou et al. 1998). Upon release to 1 atm, the spectrum reverts to that of diopside, indicating that the diopside bonds did not break and reform. Instead, the structural changes appear to involve a simple rearrangement of the atoms, as previously suggested (Stolper and Ahrens 1987). This high-pressure behavior is very similar to that observed for enstatite and wollastonite, other chain silicates (Serghiou et al. 1998), suggesting that pyroxenes can undergo profound phase transitions with very little activation energy. In contrast, pyroxenoids with longer repeat units in their silicate chains did
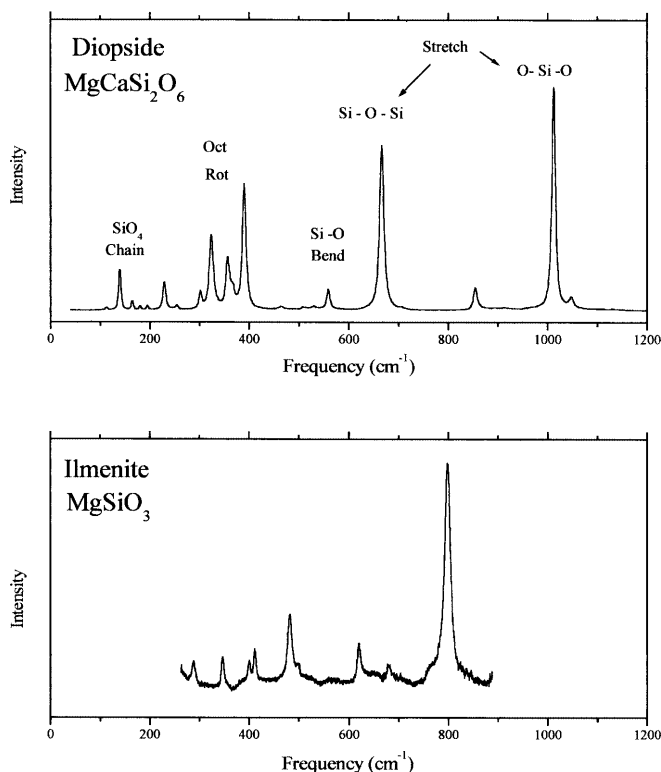
overtakes the intensity of the original peak and by 15 GPa, the original low-energy peak disappears entirely. Since the chromium fluorescence is very sensitive to the local environment of the chromium cation, this would indicate a local structural change. The primary data are presented in a sequel paper (J. Ohlert and A. Chopelas, in preparation).

At 15 GPa, the small downward shift in frequencies and change in the pressure-frequency slopes indicate there is some change in compressional mechanism. Above this pressure, there appears to be a rapid decrease in the pressure shifts of the Raman modes (Fig. 2a–d)

Fig. 5 Comparison of the ambient pressure spectra of diopside to magnesium silicate ilmenite. The ilmenite spectrum is suggestive of that found at the highest pressures in Fig. 4

not transform to a crystalline phase of higher silicon coordination, but rather became amorphous (Serghiou et al. 2000). Whether a chain silicate becomes amorphous or transforms to a denser crystalline phase upon compression appears to depend on the sequencing of the silicate chains that make up their structures. (Serghiou et al. 2000).

This last transition occurs far above the stability range expected for diopside but it is instructional to see that a silicate can change coordination at room temperature, in contrast to observations made for other silicates.

Mantle implications

On cursory examination of the changes in the Raman spectra observed at low pressures, it is expected that these changes will not have a significant impact on extrapolation of low-pressure data to mantle conditions. The Raman spectrum did not significantly change the number of modes or distribution for these changes, meaning that the thermodynamic properties for this material do not significantly change. The changes seen at 15 GPa are already almost too high in pressure to have any bearing on a particular mantle model. The change from one $C2/c$ structure to another does not appear to have a significant volume change at room temperature, as shown by the continuity of the frequency pressure function for the Raman modes. However, this will have

to be looked at more closely at mantle temperatures and high pressures. For calculation of the pressure dependence of the thermodynamic properties, presented in a subsequent paper, the effect of changing the spectrum will be examined more closely.

It is expected, then, that since orthopyroxene reverts into a high-pressure $C2/c$ clinopyroxene phase as pressure and the diopside low-pressure $C2/c$ phase becomes structurally similar with two octahedral cations, the magnesium-rich and calcium-rich pyroxenes could be one phase. It is this phase that will eventually become the garnet phase in the lower part of the transition zone. Estimates of the thermodynamics of the transformation of pyroxene to garnet need to take the high-pressure $C2/c$ phase into consideration. It is not clear what impact the addition of calcium to a high clinopyroxene structure under these conditions will have on the volume or thermoelastic properties. There is likely to be a non-ideal mixing similar to that observed for garnets.

This study does demonstrate, as with our previous spectroscopic studies (e.g., Chopelas 1999), that the properties of the low-pressure mineral phases do not continuously change as they are compressed and that simple extrapolations of their properties to mantle conditions cannot generally be made without examining them over the pressure range by a method as sensitive as Raman spectroscopy.

References

Chopelas A (1990) Thermal properties of forsterite at mantle pressures derived from vibrational spectroscopy. Phys Chem Miner 17: 149–157

Chopelas A (1991) Single-crystal Raman spectra of forsterite, fayalite, and monticellite. Am Mineral 76: 1101–1109

Chopelas A (1999) Estimates of mantle relevant Clapeyron slopes in the MgSiO₃ system from high-pressure spectroscopic data. Am Mineral 84: 233–245

Downs RT, Gibbs GV, Boisen MB, Jr (1999) Topological analysis of the $P21/c$ to $C2/c$ transition in pyroxenes as a function of temperature and pressure. EOS, Trans AGU, Fall Meeting Supp (Abstract) 80: F1140

Etchepare J (1970) Study by Raman spectroscopy of crystalline and glassy diopside. In: Douglas RW, Ellis B (eds) Amorphous materials International Conference on Noncrystalline Solids, Wiley Interscience, London, pp 337–346

Hofmeister AM, Chopelas A (1991) Vibrational spectroscopy of end-member silicate garnets. Phys Chem Miner 17: 503–526

Hugh-Jones DA, Woodland AB, Angel RJ (1994) The structure of high-pressure $C2/c$ ferrosilite and crystal chemistry of high-pressure $C2/c$ pyroxenes. Am Mineral 79: 1032–1041

Levein L, Prewitt CT (1981) High-pressure structural study of diopside. Am Mineral 66: 315–323

Levein L, Weidner DJ, Prewitt CT (1979) Elasticity of diopside. Phys Chem Miner 4: 105–113

Serghiou G, Zerr A, Chopelas A (1998) Phase transitions and disordering of CaSiO₃ upon compression. Rev High Press Sci Tech 7: 359–361

Serghiou G, Chopelas A, Boehler R (2000) Explanation of pressure-induced transformations in chain silicates based on their modular structures. J Phys: Cond Matt 12: 8939–8952

Stolper EM, Ahrens TJ (1987) On the nature of pressure-induced coordination changes in silicate melts and glasses. Geophys Res Lett 14: 1231–1233